Supporting Information

Photothermally-activated suspending aerogel triggers biphase interface reaction for high-efficiency and additive-free hydrogen generation

Qian Zhang,[1] Bo Jiang,[1] Yuming Gao,[1] Lin Li,[1,] Dawei Tang[1]*

[1]School of Energy and Power Engineering, Key Laboratory of Ocean Energy Utilization and Energy Conservation of Ministry of Education, Dalian University of Technology, 116024, China

Experimental Methods

Preparation of the Pd/rGO aerogel

Firstly, Na_2PdCl_4 (0.02 M, 4.5 mL) was added into the GO aqueous solution (1.43 mg/mL, 35.0 mL) with magnetic stirring at room temperature for 2 h. Subsequently, 4.0 g of glucose was added to the homogeneous GO solution under vigorous stirring at room temperature to obtain a uniform solution mixture. After that, the mixture was dropped into a reaction still for hydrothermal reaction (1200 min, 120℃), forming a columniform gel with a diameter of 2 cm. Finally, the gel was washed several times with distilled water and reduced by immersion in a $NaBH_4$ (100.0 mM, 1.0 mL) solution for 12 h. After 6 h of freeze-drying treatment, Pd/rGO aerogel was fabricated. It is noted that the thickness of the aerogel can be controlled by regulating the amount of glucose.

Characterizations

X-ray diffraction patterns were obtained on a Rigaku Ultima IV diffractometer with Cu Kα radiation using a current of 100 mA and a voltage of 40 kV. Scanning electron microscopy images were obtained on a field-emission scanning electron microscope (TESCAN MIRA LMS) with an accelerating voltage of 5 kV. Transmission electron microscopy mapping images were obtained on a transmission electron microscope (Tecnai F30, FEI). Solar absorption spectra were collected using a UV-vis-NIR spectrophotometer (PE Lambda1050).

Pure FA dehydrogenation test

The aerogel was cut into a circle of 1.5 cm in diameter according to the size of the lab-scale nanoreactor (Figure 4a). In a typical reaction, the aerogel is arranged above the liquid FA level, and the gas gap is set as 10 mm. Before being irradiated by a solar simulator (71S0503A, Sofn, China), N_2 was passed through the nanoreactor to drain air. An optical power meter (S310C, Thorlabs, USA) was employed to ensure the optical density of simulated solar illumination (1 kW/m^2). The generated gas product is first fed into a

condenser to wipe off the rest of the FA or water vapors. Then, the gas products were collected by gas bag and were determined by a gas chromatograph (Agilent 7890B).

Theoretical calculation

Calculations were conducted based on Density Functional Theory. The dispersion-corrected DFT-D3 schemes were employed to describe the possible Van der Waals interactions. The cut-off energy was set to be 400 eV, and the total energy convergence was set to be $<10^{-5}$ eV. According to the XRD and HRTEM characterization results, Pd (111) crystallographic planes that are easily exposed is evidenced as the main active sites. Thus, we modeled the Pd (111) surface as a 4 × 4 slab with four layers, where the top two layers were relaxed and the bottom two layers were kept fixed. Structures were considered converged when the maximum forces on all atoms were below 0.02 eV/Å. The Brillouin zone was sampled with a 3 × 3 × 1 Monkhorst-Pack k-point mesh. The periodic images were separated by 10 Å of vacuum in the c-direction to avoid periodic interactions (Figure S10). For the liquid FA dehydrogenation, we constructed the HCOOH molecule with surrounding three H_2O molecules as adsorbates adsorbed on the Pd (111) surface (Figure S11). For the gaseous FA dehydrogenation, we constructed a bimolecular hydrogen-bonded complex model (HCOOH-HCOO*) as the adsorbate adsorbed on the Pd (111) surface (Figure S12). The atomic structures were analyzed via the VESTA code. The reaction energy barrier for each elementary reaction step is evaluated using the climbing image nudged elastic band (CINEB) method with four interpolated images between the initial and final states. The transition states (TS) were similarly optimized until the forces on all atoms were below 0.05 eV/Å and were confirmed using vibrational analysis by the presence of a single imaginary mode.

Equations

Equation S1. The calculation of thermal radiation flux of the aerogel at 70℃ according to Planck's law.

$$\mu(\lambda,T)=\frac{8\pi hc}{\lambda^5}\cdot\frac{1}{e^{\frac{hc}{\lambda kT}}-1}$$

where h is Planck's constant, T is the thermodynamic temperature, and k is Boltzmann's constant.

Equation S2. The calculation of initial turnover frequency.

$$TOF=\frac{P_{atm}V_{H_2}/RT}{n_{\mathrm{Pd}}t}$$

where P_{atm} is the atmospheric pressure (101325 Pa), V_{gas} is the generated total hydrogen volume when the conversion reaches 20%, R is the universal gas content (8.314 m^3 Pa mol^{-1} K^{-1}), T is room temperature (298 K), and t is the reaction time when the conversion reaches 20%. n_{Pd} is the total mole number of Pd in the aerogel (0.0746 mg), which is obtained by the inductively coupled plasma-mass spectroscopy (ICP-MS) characterization of the aerogel.

Equation S3. The calculation of liquid FA diffusion flux (N_l) according to Fick law.

$$N_l=D_l^T\frac{c_l^{sat}}{H}$$

where D_l^T is the diffusion coefficient (1.52×10^{-9} m^2/s) of liquid FA at 298 K,[31, 32] c_g^{sat} is the saturated liquid FA concentration, and H is the diffusion distance in the BTS.

Equation S4. The calculation of gaseous FA diffusion flux (N_g) according to Fick law.

$$N_{\mathrm{g}}=D_g^T\frac{c_g^{sat}}{H}$$

where D_g^T is the diffusion coefficient at 316 K (1.20×10^{-5} m^2/s),[33] c_g^{sat} is the saturated gaseous FA concentration, and H is the diffusion distance, which is also named as the gas gap in the SBS.

Equation S5. The calculation of hydrogen gas diffusion coefficient D_L in a liquid-phase environment.

$$D_L = 7.4\times10^{-8}\frac{T(\psi M)_{\mathrm{FA}}^{0.5}}{\mu_{\mathrm{FA}}V_{H_2}^{0.6}}$$

where T is the temperature (K), ψ_{FA} (=1.33) is the "association" parameter of FA that represents the degree of the aggregation of FA molecules,[34] M_{FA} and μ denote the molecular mass and viscosity of formic acid, respectively, and V_{H2} is the molar volume of hydrogen ($cm^3\ mol^{-1}$).

Equation S6. The calculation of hydrogen gas diffusion coefficient D_G in a gas-phase environment.[35]

$$D_{\mathrm{G}} = \frac{1.86\times10^{-3} * T^{1.5}\sqrt{M_{H_2}^{-1} + M^{-1}}}{P*\sigma^2*\Omega}$$

$$\sigma = \frac{1}{2}\left(\sigma_{\mathrm{H_2}} + \sigma_{\mathrm{FA}}\right),\ \Omega = \frac{kT}{\sqrt{\varepsilon_{H_2}\varepsilon_{FA}}}$$

$$\varepsilon = 0.75\mathrm{k}T_c,\ \sigma = \frac{5}{6}\times10^{-8}V_{\mathrm{c}}^{1/3}$$

where M is the molar mass, P is the system pressure, σ is the average collision diameter, Ω is a temperature-dependent collision integral, and k is the Boltzmann constant. ε and σ are estimated using the well-known critical parameters for a given substance, where T_c and V_c are the critical temperature (K) and the critical molar volume (cm^3/mol), respectively.

Equation S7. The calculation of Gibbs free energy.

$$\Delta G = \Delta E + \Delta E_{ZPE} - T\Delta S$$

where ΔE is the HCOOH adsorption energy, ΔE_{ZPE} is the difference in zero-point energy, T is reaction temperature, and ΔS is the difference in entropy between the adsorbed species and free species in the gas phase.

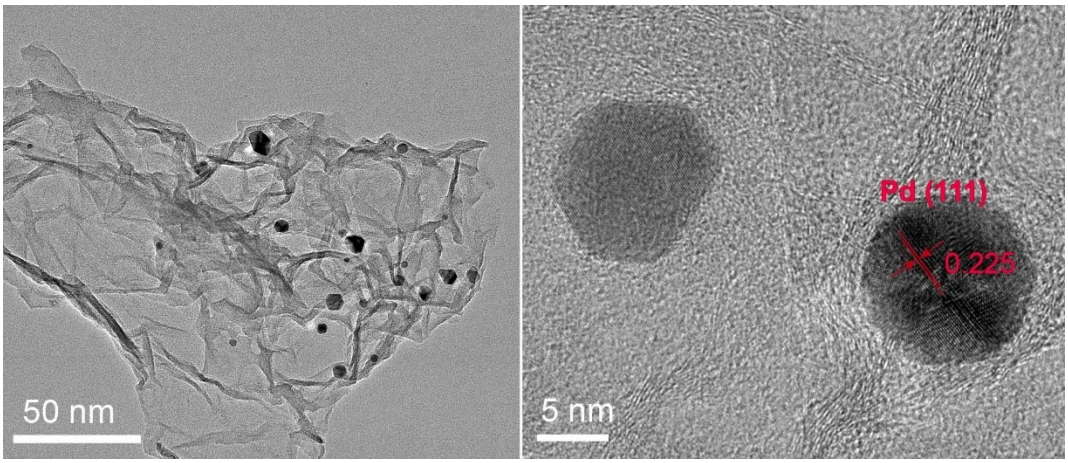

Figure S1. The TEM image of the Pd/rGO aerogel with highly dispersed Pd nanoparticles and the HRTEM image of Pd nanoparticles.

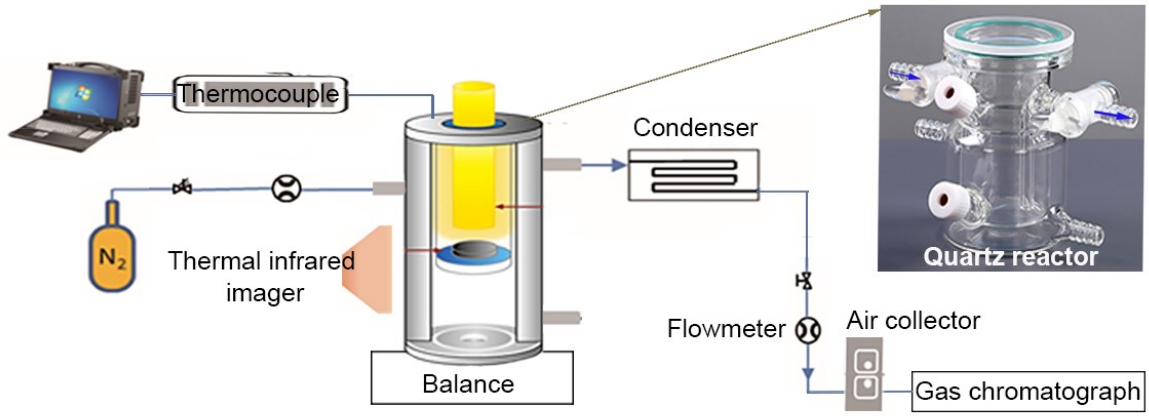

Figure S2. The experimental setup of the SBS.

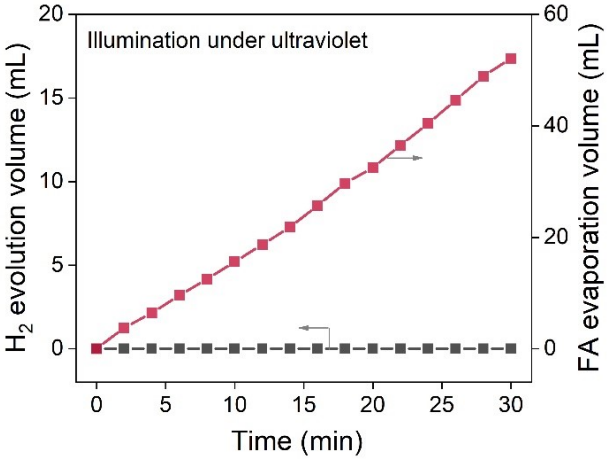

Figure S3. The H_2 evolution volume and FA evaporation volume of the Pd/rGO aerogel under ultraviolet illumination.

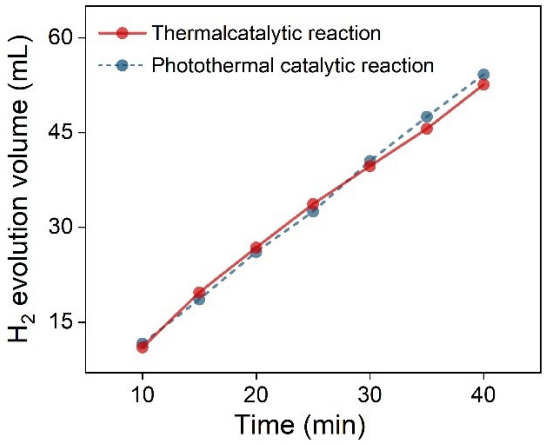

Figure S4. The H_2 evolution volume of the Pd/rGO aerogel under the conditions of thermal-driven reaction and photothermal-driven reactions.

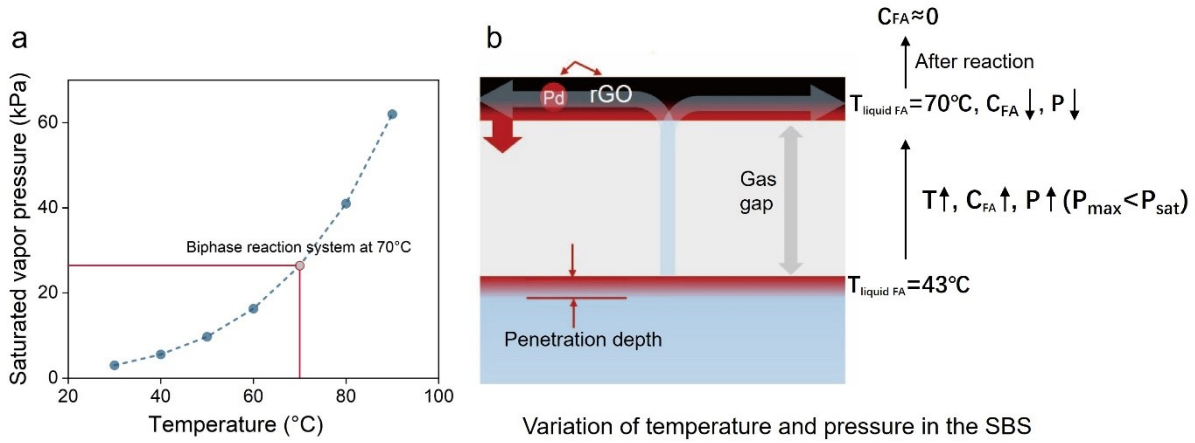

Figure S5. (a) Curve of the FA saturated vapor pressure with temperature, (b) Variation of temperature and pressure in the SBS.

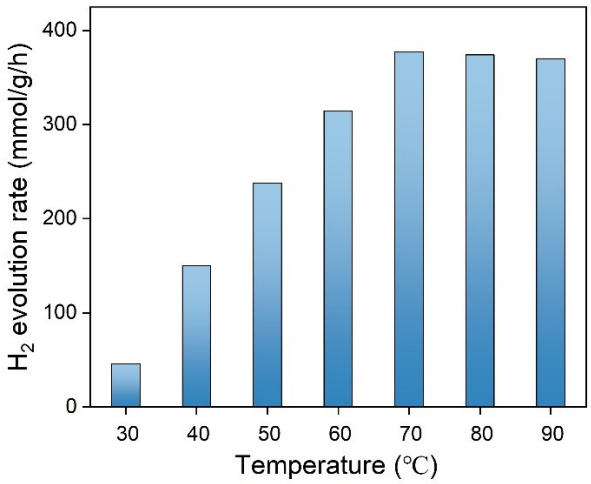

Figure S6. The H_2 evolution rate of the SBS under different reaction temperatures.

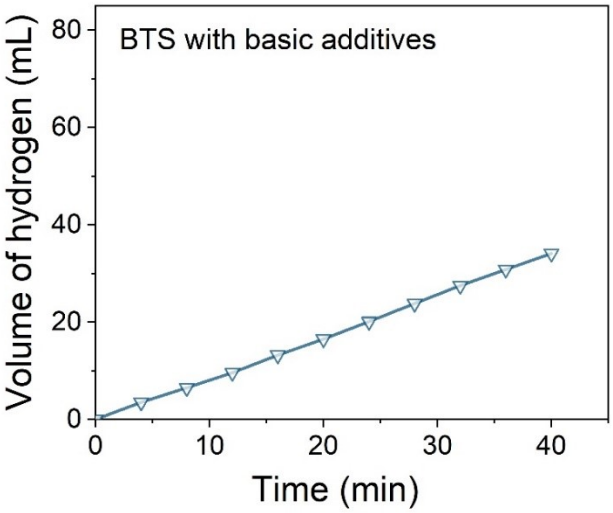

Figure S7. The hydrogen evolution performance of the BTS in the presence of liquid basic additive (HCOONa).

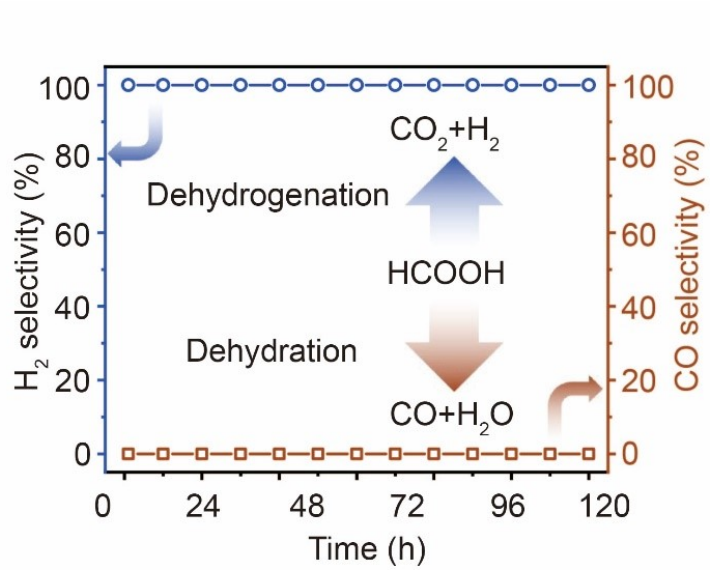

Figure S8. H_2 and CO selectivity of the SBS.

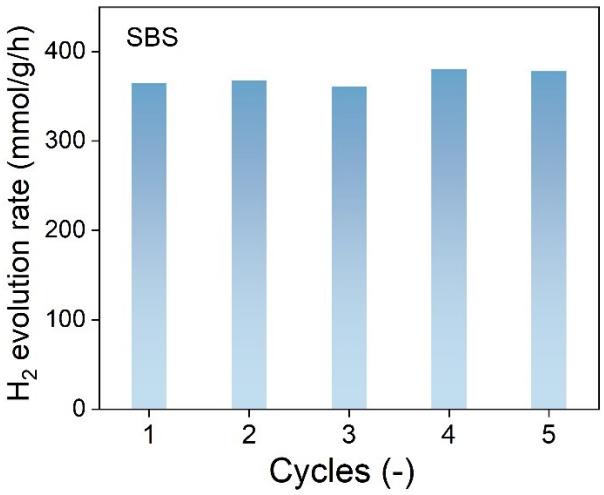

Figure S9. The H_2 evolution rate of the SBS in five cycles.

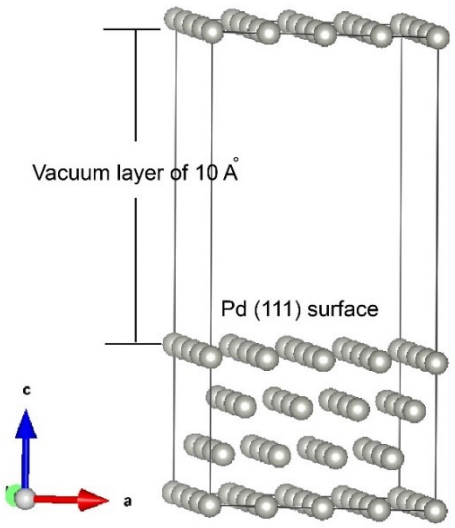

	x	y	z				
Pd1	0.00000	0.00000	0.00000	Pd36	0.00000	0.50000	0.31254
Pd2	0.33333	0.16667	0.10415	Pd37	1.00000	0.75000	0.00000
Pd3	0.16667	0.33333	0.20809	Pd38	0.33333	0.91667	0.10415
Pd4	0.00000	-0.00000	0.31254	Pd39	0.16667	0.58333	0.20809
Pd5	1.00000	0.25000	0.00000	Pd40	0.00000	0.75000	0.31254
Pd6	0.33333	0.41667	0.10415	Pd41	0.25000	0.75000	0.00000
Pd7	0.16667	0.08333	0.20809	Pd42	0.08333	0.91667	0.10415
Pd8	0.00000	0.25000	0.31254	Pd43	0.41667	0.58333	0.20809
Pd9	0.25000	0.25000	0.00000	Pd44	0.25000	0.75000	0.31254
Pd10	0.08333	0.41667	0.10415	Pd45	0.25000	0.50000	0.00000
Pd11	0.41667	0.08333	0.20809	Pd46	0.08333	0.66667	0.10415
Pd12	0.25000	0.25000	0.31254	Pd47	0.41667	0.83333	0.20809
Pd13	0.25000	0.00000	0.00000	Pd48	0.25000	0.50000	0.31254
Pd14	0.08333	0.16667	0.10415	Pd49	0.50000	0.50000	0.00000
Pd15	0.41667	0.33333	0.20809	Pd50	0.83333	0.66667	0.10415
Pd16	0.25000	-0.00000	0.31254	Pd51	0.66667	0.83333	0.20809
Pd17	0.50000	0.00000	0.00000	Pd52	0.50000	0.50000	0.31254
Pd18	0.83333	0.16667	0.10415	Pd53	0.50000	0.75000	0.00000
Pd19	0.66667	0.33333	0.20809	Pd54	0.83333	0.91667	0.10415
Pd20	0.50000	-0.00000	0.31254	Pd55	0.66667	0.58333	0.20809
Pd21	0.50000	0.25000	0.00000	Pd56	0.50000	0.75000	0.31254
Pd22	0.83333	0.41667	0.10415	Pd57	0.75000	0.75000	0.00000
Pd23	0.66667	0.08333	0.20809	Pd58	0.58333	0.91667	0.10415
Pd24	0.50000	0.25000	0.31254	Pd59	0.91667	0.58333	0.20809
Pd25	0.75000	0.25000	0.00000	Pd60	0.75000	0.75000	0.31254
Pd26	0.58333	0.41667	0.10415	Pd61	0.75000	0.50000	0.00000
Pd27	0.91667	0.08333	0.20809	Pd62	0.58333	0.66667	0.10415
Pd28	0.75000	0.25000	0.31254	Pd63	0.91667	0.83333	0.20809
Pd29	0.75000	0.00000	0.00000	Pd64	0.75000	0.50000	0.31254
Pd30	0.58333	0.16667	0.10415				
Pd31	0.91667	0.33333	0.20809				
Pd32	0.75000	-0.00000	0.31254				

Figure S10. The optimized computation model of Pd (111) surface and its atom coordinates.

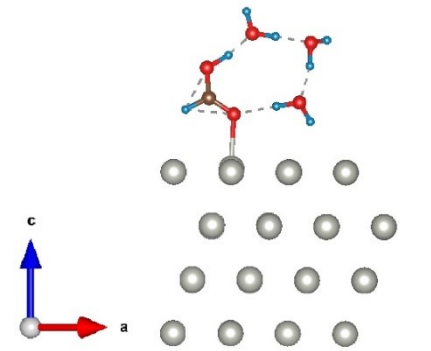

	x	y	z				
Pd1	0.00620	0.00705	0.00052	Pd38	0.33906	0.92351	0.10290
Pd2	0.33886	0.17356	0.10453	Pd39	0.17266	0.59022	0.20634
Pd3	0.17339	0.33972	0.20895	Pd40	0.00617	0.75733	0.31091
Pd4	0.00448	0.00579	0.31087	Pd41	0.25574	0.75675	0.99981
Pd5	0.00609	0.25651	0.00061	Pd42	0.08925	0.92393	0.10321
Pd6	0.33871	0.42299	0.10465	Pd43	0.42275	0.59129	0.20662
Pd7	0.17346	0.09198	0.20881	Pd44	0.25632	0.75758	0.31075
Pd8	0.00456	0.25781	0.31104	Pd45	0.25591	0.50620	0.00059
Pd9	0.25599	0.25672	0.00136	Pd46	0.08897	0.67342	0.10289
Pd10	0.08919	0.42304	0.10334	Pd47	0.42271	0.84064	0.20625
Pd11	0.42302	0.09038	0.20689	Pd48	0.25674	0.50978	0.31115
Pd12	0.25743	0.25839	0.31794	Pd49	0.50546	0.50618	0.00064
Pd13	0.25615	0.00687	0.00027	Pd50	0.83903	0.67342	0.10278
Pd14	0.08926	0.17349	0.10445	Pd51	0.67269	0.84049	0.20630
Pd15	0.42103	0.33960	0.20911	Pd52	0.50845	0.50987	0.31125
Pd16	0.25650	0.00577	0.31108	Pd53	0.50582	0.75653	0.99989
Pd17	0.50565	0.00676	0.99985	Pd54	0.83894	0.92351	0.10288
Pd18	0.83891	0.17315	0.10294	Pd55	0.67262	0.59035	0.20632
Pd19	0.67235	0.34051	0.20655	Pd56	0.50653	0.75802	0.31107
Pd20	0.50664	0.00758	0.31104	Pd57	0.75599	0.75654	0.99987
Pd21	0.50561	0.25642	0.00058	Pd58	0.58890	0.92336	0.10273
Pd22	0.83895	0.42326	0.10297	Pd59	0.92260	0.59046	0.20646
Pd23	0.67267	0.09055	0.20631	Pd60	0.75624	0.75753	0.31093
Pd24	0.50850	0.25798	0.31161	Pd61	0.75613	0.50655	0.99988
Pd25	0.75585	0.25670	0.00010	Pd62	0.58888	0.67351	0.10303
Pd26	0.58843	0.42303	0.10349	Pd63	0.92287	0.84081	0.20624
Pd27	0.92214	0.09022	0.20672	Pd64	0.75661	0.50809	0.31125
Pd28	0.75630	0.25780	0.31097	O1	0.19956	0.21137	0.41604
Pd29	0.75590	0.00657	0.99986	O2	0.35897	0.35821	0.48615
Pd30	0.58883	0.17320	0.10308	O3	0.53663	0.53332	0.41129
Pd31	0.92280	0.34036	0.20639	O4	0.74096	0.73834	0.41021
Pd32	0.75579	0.00742	0.31091	C1	0.24197	0.25114	0.46881
Pd33	0.00585	0.50669	0.00002	C2	0.64140	0.63704	0.43642
Pd34	0.33901	0.67354	0.10276	H1	0.42388	0.42035	0.45136
Pd35	0.17271	0.84089	0.20631	H2	0.17638	0.19219	0.50825
Pd36	0.00621	0.50785	0.31102	H3	0.64353	0.63630	0.48728
Pd37	0.00601	0.75660	0.99981				

Figure S11. The optimized computation model of HCOOH-H_2O molecules adsorption and its atom coordinates.

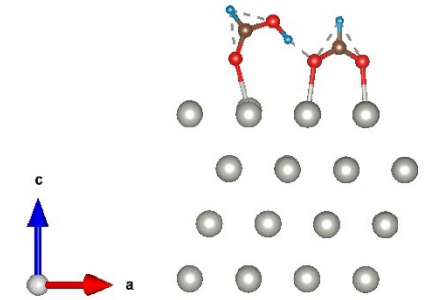

	x	y	z				
Pd1	0.00620	0.00705	0.00052	Pd38	0.33906	0.92351	0.10290
Pd2	0.33886	0.17356	0.10453	Pd39	0.17266	0.59022	0.20634
Pd3	0.17339	0.33972	0.20895	Pd40	0.00617	0.75733	0.31091
Pd4	0.00448	0.00579	0.31087	Pd41	0.25574	0.75675	0.99981
Pd5	0.00609	0.25651	0.00061	Pd42	0.08925	0.92393	0.10321
Pd6	0.33871	0.42299	0.10465	Pd43	0.42275	0.59129	0.20662
Pd7	0.17346	0.09198	0.20881	Pd44	0.25632	0.75758	0.31075
Pd8	0.00456	0.25781	0.31104	Pd45	0.25591	0.50620	0.00059
Pd9	0.25599	0.25672	0.00136	Pd46	0.08897	0.67342	0.10289
Pd10	0.08919	0.42304	0.10334	Pd47	0.42271	0.84064	0.20625
Pd11	0.42302	0.09038	0.20689	Pd48	0.25674	0.50978	0.31115
Pd12	0.25743	0.25839	0.31794	Pd49	0.50546	0.50618	0.00064
Pd13	0.25615	0.00687	0.00027	Pd50	0.83903	0.67342	0.10278
Pd14	0.08926	0.17349	0.10445	Pd51	0.67269	0.84049	0.20630
Pd15	0.42103	0.33960	0.20911	Pd52	0.50845	0.50987	0.31125
Pd16	0.25650	0.00577	0.31108	Pd53	0.50582	0.75653	0.99989
Pd17	0.50565	0.00676	0.99985	Pd54	0.83894	0.92351	0.10288
Pd18	0.83891	0.17315	0.10294	Pd55	0.67262	0.59035	0.20632
Pd19	0.67235	0.34051	0.20655	Pd56	0.50653	0.75802	0.31107
Pd20	0.50664	0.00758	0.31104	Pd57	0.75599	0.75654	0.99987
Pd21	0.50561	0.25642	0.00058	Pd58	0.58890	0.92336	0.10273
Pd22	0.83895	0.42326	0.10297	Pd59	0.92260	0.59046	0.20646
Pd23	0.67267	0.09055	0.20631	Pd60	0.75624	0.75753	0.31093
Pd24	0.50850	0.25798	0.31161	Pd61	0.75613	0.50655	0.99988
Pd25	0.75585	0.25670	0.00010	Pd62	0.58888	0.67351	0.10303
Pd26	0.58843	0.42303	0.10349	Pd63	0.92287	0.84081	0.20624
Pd27	0.92214	0.09022	0.20672	Pd64	0.75661	0.50809	0.31125
Pd28	0.75630	0.25780	0.31097	O1	0.19956	0.21137	0.41604
Pd29	0.75590	0.00657	0.99986	O2	0.35897	0.35821	0.48615
Pd30	0.58883	0.17320	0.10308	O3	0.53663	0.53332	0.41129
Pd31	0.92280	0.34036	0.20639	O4	0.74096	0.73834	0.41021
Pd32	0.75579	0.00742	0.31091	C1	0.24197	0.25114	0.46881
Pd33	0.00585	0.50669	0.00002	C2	0.64140	0.63704	0.43642
Pd34	0.33901	0.67354	0.10276	H1	0.42388	0.42035	0.45136
Pd35	0.17271	0.84089	0.20631	H2	0.17638	0.19219	0.50825
Pd36	0.00621	0.50785	0.31102	H3	0.64353	0.63630	0.48728
Pd37	0.00601	0.75660	0.99981				

Figure S12. The optimized computation model of HCOOH-HCOO complexes adsorption and its atom coordinates.

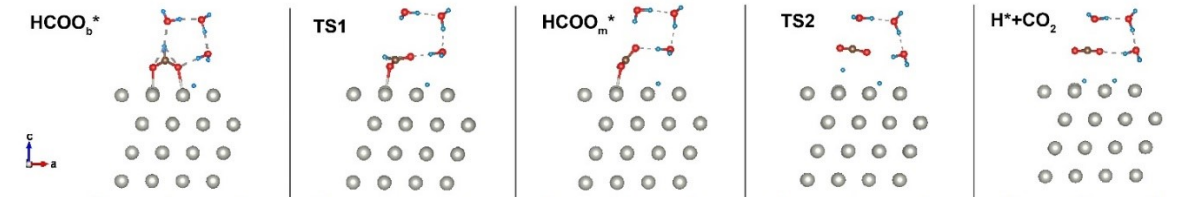

	HCOO$_b$*			TS1			HCOO$_m$*			TS2			H*+CO$_2$		
	x	y	z	x	y	z	x	y	z	x	y	z	x	y	z
Pd1	0.00621	0.00706	0.00052	0.00621	0.00706	0.00052	0.00621	0.00706	0.00052	0.00621	0.00706	0.00052	0.00621	0.00706	0.00052
Pd2	0.33886	0.17356	0.10453	0.33886	0.17356	0.10453	0.33886	0.17356	0.10453	0.33886	0.17356	0.10453	0.33886	0.17356	0.10453
Pd3	0.17339	0.33972	0.20895	0.17339	0.33972	0.20895	0.17339	0.33972	0.20895	0.17339	0.33972	0.20895	0.17339	0.33972	0.20895
Pd4	0.00448	0.00579	0.31087	0.00448	0.00579	0.31087	0.00448	0.00579	0.31087	0.00448	0.00579	0.31087	0.00448	0.00579	0.31087
Pd5	0.00609	0.25651	0.00060	0.00609	0.25651	0.00060	0.00609	0.25651	0.00060	0.00609	0.25651	0.00060	0.00609	0.25651	0.00060
Pd6	0.33871	0.42299	0.10465	0.33871	0.42299	0.10465	0.33871	0.42299	0.10465	0.33871	0.42299	0.10465	0.33871	0.42299	0.10465
Pd7	0.17346	0.09198	0.20881	0.17346	0.09198	0.20881	0.17346	0.09198	0.20881	0.17346	0.09198	0.20881	0.17346	0.09198	0.20881
Pd8	0.00456	0.25781	0.31104	0.00456	0.25781	0.31104	0.00456	0.25781	0.31104	0.00456	0.25781	0.31104	0.00456	0.25781	0.31104
Pd9	0.25599	0.25672	0.00136	0.25599	0.25672	0.00136	0.25599	0.25672	0.00136	0.25599	0.25672	0.00136	0.25599	0.25672	0.00136
Pd10	0.08919	0.42304	0.10334	0.08919	0.42304	0.10334	0.08919	0.42304	0.10334	0.08919	0.42304	0.10334	0.08919	0.42304	0.10334
Pd11	0.42302	0.09038	0.20689	0.42302	0.09038	0.20689	0.42302	0.09038	0.20689	0.42302	0.09038	0.20689	0.42302	0.09038	0.20689
Pd12	0.25743	0.25839	0.31794	0.25743	0.25839	0.31794	0.25743	0.25839	0.31794	0.25743	0.25839	0.31794	0.25743	0.25839	0.31794
Pd13	0.25615	0.00687	0.00027	0.25615	0.00687	0.00027	0.25615	0.00687	0.00027	0.25615	0.00687	0.00027	0.25615	0.00687	0.00027
Pd14	0.08926	0.17349	0.10445	0.08926	0.17349	0.10445	0.08926	0.17349	0.10445	0.08926	0.17349	0.10445	0.08926	0.17349	0.10445
Pd15	0.42103	0.33960	0.20911	0.42103	0.33960	0.20911	0.42103	0.33960	0.20911	0.42103	0.33960	0.20911	0.42103	0.33960	0.20911
Pd16	0.25650	0.00577	0.31108	0.25650	0.00577	0.31108	0.25650	0.00577	0.31108	0.25650	0.00577	0.31108	0.25650	0.00577	0.31108
Pd17	0.50588	0.00669	0.99985	0.50582	0.00669	0.99990	0.50596	0.00673	0.99994	0.50585	0.00663	0.99991	0.50590	0.00670	0.99996
Pd18	0.83891	0.17315	0.10294	0.83891	0.17315	0.10294	0.83891	0.17315	0.10294	0.83891	0.17315	0.10294	0.83891	0.17315	0.10294
Pd19	0.67235	0.34051	0.20655	0.67235	0.34051	0.20655	0.67235	0.34051	0.20655	0.67235	0.34051	0.20655	0.67235	0.34051	0.20655
Pd20	0.50664	0.00758	0.31104	0.50664	0.00758	0.31104	0.50664	0.00758	0.31104	0.50664	0.00758	0.31104	0.50664	0.00758	0.31104
Pd21	0.50561	0.25642	0.00059	0.50561	0.25642	0.00059	0.50561	0.25642	0.00059	0.50561	0.25642	0.00059	0.50561	0.25642	0.00059
Pd22	0.83895	0.42326	0.10297	0.83895	0.42326	0.10297	0.83895	0.42326	0.10297	0.83895	0.42326	0.10297	0.83895	0.42326	0.10297
Pd23	0.67267	0.09055	0.20631	0.67267	0.09055	0.20631	0.67267	0.09055	0.20631	0.67267	0.09055	0.20631	0.67267	0.09055	0.20631
Pd24	0.50850	0.25798	0.31161	0.50850	0.25798	0.31161	0.50850	0.25798	0.31161	0.50850	0.25798	0.31161	0.50850	0.25798	0.31161
Pd25	0.75585	0.25670	0.00010	0.75585	0.25670	0.00010	0.75585	0.25670	0.00010	0.75585	0.25670	0.00010	0.75585	0.25670	0.00010
Pd26	0.58843	0.42303	0.10349	0.58843	0.42303	0.10349	0.58843	0.42303	0.10349	0.58843	0.42303	0.10349	0.58843	0.42303	0.10349
Pd27	0.92214	0.09022	0.20672	0.92214	0.09022	0.20672	0.92214	0.09022	0.20672	0.92214	0.09022	0.20672	0.92214	0.09022	0.20672
Pd28	0.75630	0.25780	0.31097	0.75630	0.25780	0.31097	0.75630	0.25780	0.31097	0.75630	0.25780	0.31097	0.75630	0.25780	0.31097
Pd29	0.75605	0.00660	0.99983	0.75591	0.00667	0.99987	0.75607	0.00662	0.99985	0.75582	0.00669	0.99987	0.75573	0.00665	0.99987
Pd30	0.58883	0.17320	0.10308	0.58883	0.17320	0.10308	0.58883	0.17320	0.10308	0.58883	0.17320	0.10308	0.58883	0.17320	0.10308
Pd31	0.92280	0.34036	0.20639	0.92280	0.34036	0.20639	0.92280	0.34036	0.20639	0.92280	0.34036	0.20639	0.92280	0.34036	0.20639
Pd32	0.75579	0.00742	0.31091	0.75579	0.00742	0.31091	0.75579	0.00742	0.31091	0.75579	0.00742	0.31091	0.75579	0.00742	0.31091
Pd33	0.00585	0.50669	0.00002	0.00585	0.50669	0.00002	0.00585	0.50669	0.00002	0.00585	0.50669	0.00002	0.00585	0.50669	0.00002
Pd34	0.33901	0.67354	0.10276	0.33901	0.67354	0.10276	0.33901	0.67354	0.10276	0.33901	0.67354	0.10276	0.33901	0.67354	0.10276
Pd35	0.17271	0.84089	0.20631	0.17271	0.84089	0.20631	0.17271	0.84089	0.20631	0.17271	0.84089	0.20631	0.17271	0.84089	0.20631
Pd36	0.00621	0.50785	0.31102	0.00621	0.50785	0.31102	0.00621	0.50785	0.31102	0.00621	0.50785	0.31102	0.00621	0.50785	0.31102
Pd37	0.00599	0.75658	0.99971	0.00567	0.75643	0.99979	0.00560	0.75643	0.99979	0.00568	0.75695	0.99992	0.00579	0.75662	0.99995
Pd38	0.33906	0.92351	0.10290	0.33906	0.92351	0.10290	0.33906	0.92351	0.10290	0.33906	0.92351	0.10290	0.33906	0.92351	0.10290
Pd39	0.17266	0.59022	0.20634	0.17266	0.59022	0.20634	0.17266	0.59022	0.20634	0.17266	0.59022	0.20634	0.17266	0.59022	0.20634
Pd40	0.00617	0.75733	0.31091	0.00617	0.75733	0.31091	0.00617	0.75733	0.31091	0.00617	0.75733	0.31091	0.00617	0.75733	0.31091
Pd41	0.25586	0.75664	0.99980	0.25568	0.75656	0.99989	0.25584	0.75664	0.99988	0.25574	0.75659	0.99986	0.25572	0.75656	0.99987
Pd42	0.08925	0.92393	0.10321	0.08925	0.92393	0.10321	0.08925	0.92393	0.10321	0.08925	0.92393	0.10321	0.08925	0.92393	0.10321
Pd43	0.42275	0.59129	0.20662	0.42275	0.59129	0.20662	0.42275	0.59129	0.20662	0.42275	0.59129	0.20662	0.42275	0.59129	0.20662
Pd44	0.25632	0.75758	0.31075	0.25632	0.75758	0.31075	0.25632	0.75758	0.31075	0.25632	0.75758	0.31075	0.25632	0.75758	0.31075
Pd45	0.25591	0.50620	0.00059	0.25591	0.50620	0.00059	0.25591	0.50620	0.00059	0.25591	0.50620	0.00059	0.25591	0.50620	0.00059
Pd46	0.08897	0.67342	0.10289	0.08897	0.67342	0.10289	0.08897	0.67342	0.10289	0.08897	0.67342	0.10289	0.08897	0.67342	0.10289
Pd47	0.42271	0.84064	0.20625	0.42271	0.84064	0.20625	0.42271	0.84064	0.20625	0.42271	0.84064	0.20625	0.42271	0.84064	0.20625
Pd48	0.25674	0.50978	0.31115	0.25674	0.50978	0.31115	0.25674	0.50978	0.31115	0.25674	0.50978	0.31115	0.25674	0.50978	0.31115
Pd49	0.50546	0.50618	0.00064	0.50546	0.50618	0.00064	0.50546	0.50618	0.00064	0.50546	0.50618	0.00064	0.50546	0.50618	0.00064
Pd50	0.83903	0.67342	0.10278	0.83903	0.67342	0.10278	0.83903	0.67342	0.10278	0.83903	0.67342	0.10278	0.83903	0.67342	0.10278
Pd51	0.67269	0.84049	0.20630	0.67269	0.84049	0.20630	0.67269	0.84049	0.20630	0.67269	0.84049	0.20630	0.67269	0.84049	0.20630
Pd52	0.50845	0.50987	0.31125	0.50845	0.50987	0.31125	0.50845	0.50987	0.31125	0.50845	0.50987	0.31125	0.50845	0.50987	0.31125
Pd53	0.50596	0.75653	0.99987	0.50587	0.75644	0.99989	0.50590	0.75649	0.99992	0.50595	0.75649	0.99987	0.50598	0.75643	0.99990
Pd54	0.83894	0.92351	0.10288	0.83894	0.92351	0.10288	0.83894	0.92351	0.10288	0.83894	0.92351	0.10288	0.83894	0.92351	0.10288
Pd55	0.67262	0.59035	0.20632	0.67262	0.59035	0.20632	0.67262	0.59035	0.20632	0.67262	0.59035	0.20632	0.67262	0.59035	0.20632
Pd56	0.50653	0.75802	0.31107	0.50653	0.75802	0.31107	0.50653	0.75802	0.31107	0.50653	0.75802	0.31107	0.50653	0.75802	0.31107
Pd57	0.75586	0.75652	0.00003	0.75587	0.75652	0.00003	0.75587	0.75652	0.00003	0.75587	0.75652	0.00003	0.75587	0.75652	0.00003
Pd58	0.58890	0.92336	0.10273	0.58890	0.92336	0.10273	0.58890	0.92336	0.10273	0.58890	0.92336	0.10273	0.58890	0.92336	0.10273
Pd59	0.92260	0.59046	0.20646	0.92260	0.59046	0.20646	0.92260	0.59046	0.20646	0.92260	0.59046	0.20646	0.92260	0.59046	0.20646
Pd60	0.75624	0.75753	0.31093	0.75624	0.75753	0.31093	0.75624	0.75753	0.31093	0.75624	0.75753	0.31093	0.75624	0.75753	0.31093
Pd61	0.75591	0.50641	0.00006	0.75591	0.50641	0.00006	0.75591	0.50641	0.00006	0.75591	0.50641	0.00006	0.75591	0.50641	0.00006
Pd62	0.58888	0.67351	0.10303	0.58888	0.67351	0.10303	0.58888	0.67351	0.10303	0.58888	0.67351	0.10303	0.58888	0.67351	0.10303
Pd63	0.92287	0.84081	0.20624	0.92287	0.84081	0.20624	0.92287	0.84081	0.20624	0.92287	0.84081	0.20624	0.92287	0.84081	0.20624
Pd64	0.75661	0.50809	0.31125	0.75661	0.50809	0.31125	0.75661	0.50809	0.31125	0.75661	0.50809	0.31125	0.75661	0.50809	0.31125
O1	0.65724	0.47912	0.58624	0.69893	0.49939	0.58973	0.72459	0.50787	0.59489	0.70880	0.48677	0.57100	0.71015	0.48902	0.57444
O2	0.37873	0.39121	0.57974	0.40762	0.36402	0.60201	0.43124	0.37558	0.60755	0.42480	0.39582	0.58363	0.42997	0.40300	0.57551
O3	0.71230	0.51490	0.46209	0.71092	0.51959	0.46187	0.69060	0.52539	0.46787	0.79050	0.62214	0.45396	0.76966	0.60501	0.45851
O4	0.26122	0.28972	0.41208	0.29368	0.28646	0.41065	0.29694	0.29468	0.41028	0.26999	0.33097	0.47436	0.26358	0.31883	0.45956
O5	0.46520	0.49729	0.41384	0.45610	0.49950	0.44505	0.41510	0.47570	0.47414	0.48832	0.54881	0.45985	0.46984	0.53476	0.45605
H1	0.72075	0.56879	0.60427	0.75599	0.58859	0.60948	0.77698	0.59730	0.61510	0.76566	0.55515	0.60167	0.76610	0.56323	0.60303
H2	0.68225	0.48950	0.54195	0.71461	0.51697	0.54505	0.72821	0.52853	0.55055	0.74666	0.53135	0.53093	0.74162	0.52992	0.53303
H3	0.47879	0.42555	0.58757	0.51015	0.41422	0.59957	0.53336	0.41976	0.60748	0.52549	0.42828	0.58185	0.53015	0.43233	0.57833
H4	0.34320	0.41252	0.61629	0.38143	0.42611	0.58256	0.40991	0.40083	0.56787	0.37905	0.29496	0.58691	0.38113	0.30940	0.59197
H5	0.63091	0.51806	0.44606	0.61645	0.50554	0.45450	0.59282	0.50328	0.46989	0.70562	0.62303	0.44344	0.67919	0.59250	0.44693
H6	0.71196	0.43821	0.44024	0.70390	0.43175	0.45038	0.68555	0.43585	0.45386	0.81458	0.59185	0.41568	0.79853	0.57117	0.42309
H7	0.59462	0.41960	0.34621	0.59142	0.42369	0.34699	0.59126	0.42467	0.34774	0.59099	0.42452	0.34789	0.58991	0.42392	0.34851
H8	0.35173	0.39611	0.48947	0.24985	0.43335	0.44300	0.28229	0.47304	0.40818	0.29394	0.51354	0.39635	0.34054	0.67555	0.34905
C1	0.35957	0.39515	0.43840	0.33446	0.40989	0.43268	0.33323	0.41734	0.43146	0.37159	0.42832	0.47166	0.36778	0.42584	0.46019

Figure S13. The atom coordinates of computation models in the Figure 4e.

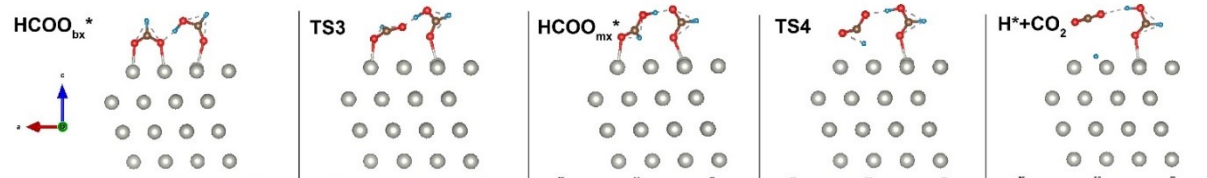

	HCOO$_{bx}$*			TS3			HCOO$_{mx}$*			TS4			H*+CO$_2$		
	x	y	z	x	y	z	x	y	z	x	y	z	x	y	z
Pd1	0.00620	0.00705	0.00052	0.00620	0.00706	0.00052	0.00620	0.00706	0.00052	0.00620	0.00706	0.00052	0.00620	0.00706	0.00052
Pd2	0.33886	0.17356	0.10453	0.33886	0.17356	0.10453	0.33886	0.17356	0.10453	0.33886	0.17356	0.10453	0.33886	0.17356	0.10453
Pd3	0.17339	0.33972	0.20895	0.17339	0.33972	0.20895	0.17339	0.33972	0.20895	0.17339	0.33972	0.20895	0.17339	0.33972	0.20895
Pd4	0.00448	0.00579	0.31087	0.00448	0.00579	0.31087	0.00448	0.00579	0.31087	0.00448	0.00579	0.31087	0.00448	0.00579	0.31087
Pd5	0.00609	0.25651	0.00061	0.00609	0.25651	0.00060	0.00609	0.25651	0.00060	0.00609	0.25651	0.00060	0.00609	0.25651	0.00060
Pd6	0.33871	0.42299	0.10465	0.33871	0.42299	0.10465	0.33871	0.42299	0.10465	0.33871	0.42299	0.10465	0.33871	0.42299	0.10465
Pd7	0.17346	0.09198	0.20881	0.17346	0.09198	0.20881	0.17346	0.09198	0.20881	0.17346	0.09198	0.20881	0.17346	0.09198	0.20881
Pd8	0.00456	0.25781	0.31104	0.00456	0.25781	0.31104	0.00456	0.25781	0.31104	0.00456	0.25781	0.31104	0.00456	0.25781	0.31104
Pd9	0.25599	0.25672	0.00136	0.25599	0.25672	0.00136	0.25599	0.25672	0.00136	0.25599	0.25672	0.00136	0.25599	0.25672	0.00136
Pd10	0.08919	0.42304	0.10334	0.08919	0.42304	0.10334	0.08919	0.42304	0.10334	0.08919	0.42304	0.10334	0.08919	0.42304	0.10334
Pd11	0.42302	0.09038	0.20689	0.42302	0.09038	0.20689	0.42302	0.09038	0.20689	0.42302	0.09038	0.20689	0.42302	0.09038	0.20689
Pd12	0.25743	0.25839	0.31794	0.25743	0.25839	0.31794	0.25743	0.25839	0.31794	0.25743	0.25839	0.31794	0.25743	0.25839	0.31794
Pd13	0.25615	0.00687	0.00027	0.25615	0.00687	0.00027	0.25615	0.00687	0.00027	0.25615	0.00687	0.00027	0.25615	0.00687	0.00027
Pd14	0.08926	0.17349	0.10445	0.08926	0.17349	0.10445	0.08926	0.17349	0.10445	0.08926	0.17349	0.10445	0.08926	0.17349	0.10445
Pd15	0.42103	0.33960	0.20911	0.42103	0.33960	0.20911	0.42103	0.33960	0.20911	0.42103	0.33960	0.20911	0.42103	0.33960	0.20911
Pd16	0.25650	0.00577	0.31108	0.25650	0.00577	0.31108	0.25650	0.00577	0.31108	0.25650	0.00577	0.31108	0.25650	0.00577	0.31108
Pd17	0.50565	0.00676	0.99985	0.50565	0.00669	0.99980	0.50572	0.00679	0.99981	0.50564	0.00667	0.99984	0.50621	0.00674	-0.00007
Pd18	0.83891	0.17315	0.10294	0.83891	0.17315	0.10294	0.83891	0.17315	0.10294	0.83891	0.17315	0.10294	0.83891	0.17315	0.10294
Pd19	0.67235	0.34051	0.20655	0.67235	0.34051	0.20655	0.67235	0.34051	0.20655	0.67235	0.34051	0.20655	0.67235	0.34051	0.20655
Pd20	0.50664	0.00758	0.31104	0.50664	0.00758	0.31104	0.50664	0.00758	0.31104	0.50664	0.00758	0.31104	0.50664	0.00758	0.31104
Pd21	0.50561	0.25642	0.00058	0.50561	0.25642	0.00058	0.50561	0.25642	0.00058	0.50561	0.25642	0.00058	0.50561	0.25642	0.00058
Pd22	0.83895	0.42326	0.10297	0.83895	0.42326	0.10297	0.83895	0.42326	0.10297	0.83895	0.42326	0.10297	0.83895	0.42326	0.10297
Pd23	0.67267	0.09055	0.20631	0.67267	0.09055	0.20631	0.67267	0.09055	0.20631	0.67267	0.09055	0.20631	0.67267	0.09055	0.20631
Pd24	0.50850	0.25798	0.31161	0.50850	0.25798	0.31161	0.50850	0.25798	0.31161	0.50850	0.25798	0.31161	0.50850	0.25798	0.31161
Pd25	0.75585	0.25670	0.00010	0.75585	0.25670	0.00010	0.75585	0.25670	0.00010	0.75585	0.25670	0.00010	0.75585	0.25670	0.00010
Pd26	0.58843	0.42303	0.10349	0.58843	0.42303	0.10349	0.58843	0.42303	0.10349	0.58843	0.42303	0.10349	0.58843	0.42303	0.10349
Pd27	0.92214	0.09022	0.20672	0.92214	0.09022	0.20672	0.92214	0.09022	0.20672	0.92214	0.09022	0.20672	0.92214	0.09022	0.20672
Pd28	0.75630	0.25780	0.31097	0.75630	0.25780	0.31097	0.75630	0.25780	0.31097	0.75630	0.25780	0.31097	0.75630	0.25780	0.31097
Pd29	0.75590	0.00657	0.99986	0.75588	0.00672	0.99987	0.75601	0.00667	0.99984	0.75584	0.00661	0.99989	0.75587	0.00645	0.99990
Pd30	0.58883	0.17320	0.10308	0.58883	0.17320	0.10308	0.58883	0.17320	0.10308	0.58883	0.17320	0.10308	0.58883	0.17320	0.10308
Pd31	0.92280	0.34036	0.20639	0.92280	0.34036	0.20639	0.92280	0.34036	0.20639	0.92280	0.34036	0.20639	0.92280	0.34036	0.20639
Pd32	0.75579	0.00742	0.31091	0.75579	0.00742	0.31091	0.75579	0.00742	0.31091	0.75579	0.00742	0.31091	0.75579	0.00742	0.31091
Pd33	0.00585	0.50669	0.00002	0.00585	0.50669	0.00002	0.00585	0.50669	0.00002	0.00585	0.50669	0.00002	0.00585	0.50669	0.00002
Pd34	0.33901	0.67354	0.10276	0.33901	0.67354	0.10276	0.33901	0.67354	0.10276	0.33901	0.67354	0.10276	0.33901	0.67354	0.10276
Pd35	0.17271	0.84089	0.20631	0.17271	0.84089	0.20631	0.17271	0.84089	0.20631	0.17271	0.84089	0.20631	0.17271	0.84089	0.20631
Pd36	0.00621	0.50785	0.31102	0.00621	0.50785	0.31102	0.00621	0.50785	0.31102	0.00621	0.50785	0.31102	0.00621	0.50785	0.31102
Pd37	0.00601	0.75660	0.99981	0.00570	0.75640	0.99980	0.00578	0.75635	0.99978	0.00582	0.75648	0.99978	0.00575	0.75647	0.99984
Pd38	0.33906	0.92351	0.10290	0.33906	0.92351	0.10290	0.33906	0.92351	0.10290	0.33906	0.92351	0.10290	0.33906	0.92351	0.10290
Pd39	0.17266	0.59022	0.20634	0.17266	0.59022	0.20634	0.17266	0.59022	0.20634	0.17266	0.59022	0.20634	0.17266	0.59022	0.20634
Pd40	0.00617	0.75733	0.31091	0.00617	0.75733	0.31091	0.00617	0.75733	0.31091	0.00617	0.75733	0.31091	0.00617	0.75733	0.31091
Pd41	0.25574	0.75675	0.99981	0.25563	0.75658	0.99992	0.25587	0.75674	0.99987	0.25558	0.75669	0.99981	0.25581	0.75643	0.99986
Pd42	0.08925	0.92393	0.10321	0.08925	0.92393	0.10321	0.08925	0.92393	0.10321	0.08925	0.92393	0.10321	0.08925	0.92393	0.10321
Pd43	0.42275	0.59129	0.20662	0.42275	0.59129	0.20662	0.42275	0.59129	0.20662	0.42275	0.59129	0.20662	0.42275	0.59129	0.20662
Pd44	0.25632	0.75758	0.31075	0.25632	0.75758	0.31075	0.25632	0.75758	0.31075	0.25632	0.75758	0.31075	0.25632	0.75758	0.31075
Pd45	0.25591	0.50620	0.00059	0.25591	0.50620	0.00059	0.25591	0.50620	0.00059	0.25591	0.50620	0.00059	0.25591	0.50620	0.00059
Pd46	0.08897	0.67342	0.10289	0.08897	0.67342	0.10289	0.08897	0.67342	0.10289	0.08897	0.67342	0.10289	0.08897	0.67342	0.10289
Pd47	0.42271	0.84064	0.20625	0.42271	0.84064	0.20625	0.42271	0.84064	0.20625	0.42271	0.84064	0.20625	0.42271	0.84064	0.20625
Pd48	0.25674	0.50978	0.31115	0.25674	0.50978	0.31115	0.25674	0.50978	0.31115	0.25674	0.50978	0.31115	0.25674	0.50978	0.31115
Pd49	0.50546	0.50618	0.00064	0.50546	0.50618	0.00064	0.50546	0.50618	0.00064	0.50546	0.50618	0.00064	0.50546	0.50618	0.00064
Pd50	0.83903	0.67342	0.10278	0.83903	0.67342	0.10278	0.83903	0.67342	0.10278	0.83903	0.67342	0.10278	0.83903	0.67342	0.10278
Pd51	0.67269	0.84049	0.20630	0.67269	0.84049	0.20630	0.67269	0.84049	0.20630	0.67269	0.84049	0.20630	0.67269	0.84049	0.20630
Pd52	0.50845	0.50987	0.31125	0.50845	0.50987	0.31125	0.50845	0.50987	0.31125	0.50845	0.50987	0.31125	0.50845	0.50987	0.31125
Pd53	0.50582	0.75653	0.99989	0.50570	0.75639	0.99985	0.50582	0.75651	0.99989	0.50570	0.75645	0.99988	0.50590	0.75650	0.99989
Pd54	0.83894	0.92351	0.10288	0.83894	0.92351	0.10288	0.83894	0.92351	0.10288	0.83894	0.92351	0.10288	0.83894	0.92351	0.10288
Pd55	0.67262	0.59035	0.20632	0.67262	0.59035	0.20632	0.67262	0.59035	0.20632	0.67262	0.59035	0.20632	0.67262	0.59035	0.20632
Pd56	0.50653	0.75802	0.31107	0.50653	0.75802	0.31107	0.50653	0.75802	0.31107	0.50653	0.75802	0.31107	0.50653	0.75802	0.31107
Pd57	0.75599	0.75654	0.99987	0.75572	0.75649	0.99988	0.75592	0.75655	0.99986	0.75574	0.75647	0.99989	0.75606	0.75639	-0.00000
Pd58	0.58890	0.92336	0.10273	0.58890	0.92336	0.10273	0.58890	0.92336	0.10273	0.58890	0.92336	0.10273	0.58890	0.92336	0.10273
Pd59	0.92260	0.59046	0.20646	0.92260	0.59046	0.20646	0.92260	0.59046	0.20646	0.92260	0.59046	0.20646	0.92260	0.59046	0.20646
Pd60	0.75624	0.75753	0.31093	0.75624	0.75753	0.31093	0.75624	0.75753	0.31093	0.75624	0.75753	0.31093	0.75624	0.75753	0.31093
Pd61	0.75613	0.50655	0.99988	0.75595	0.50647	0.99997	0.75582	0.50641	0.00003	0.75582	0.50641	0.00003	0.75582	0.50641	0.00003
Pd62	0.58888	0.67351	0.10303	0.58888	0.67351	0.10303	0.58888	0.67351	0.10303	0.58888	0.67351	0.10303	0.58888	0.67351	0.10303
Pd63	0.92287	0.84081	0.20624	0.92287	0.84081	0.20624	0.92287	0.84081	0.20624	0.92287	0.84081	0.20624	0.92287	0.84081	0.20624
Pd64	0.75661	0.50809	0.31125	0.75661	0.50809	0.31125	0.75661	0.50809	0.31125	0.75661	0.50809	0.31125	0.75661	0.50809	0.31125
O1	0.19956	0.21137	0.41604	0.31047	0.28636	0.41445	0.33487	0.32547	0.40744	0.31011	0.30294	0.41560	0.28813	0.27804	0.42054
O2	0.35897	0.35821	0.48615	0.33246	0.40457	0.50127	0.33858	0.41021	0.50078	0.30160	0.39555	0.50599	0.24931	0.34439	0.51259
O3	0.53663	0.53332	0.41129	0.51866	0.61165	0.44644	0.56286	0.62434	0.48263	0.56787	0.58791	0.48442	0.55268	0.54810	0.49093
O4	0.74096	0.73834	0.41021	0.73248	0.74738	0.40727	0.72422	0.74004	0.41123	0.74118	0.74989	0.42302	0.75005	0.75934	0.46437
C1	0.24197	0.25114	0.46881	0.26690	0.29785	0.46555	0.27491	0.32946	0.45705	0.24376	0.31060	0.45974	0.20746	0.27570	0.45974
C2	0.64140	0.63704	0.43642	0.63884	0.63559	0.43277	0.62584	0.62935	0.43241	0.63306	0.63985	0.43649	0.65135	0.65384	0.47725
H1	0.42388	0.42035	0.45136	0.41920	0.48928	0.47795	0.46871	0.52304	0.49008	0.40469	0.46087	0.49779	0.35195	0.39876	0.51229
H2	0.17638	0.19219	0.50825	0.16811	0.21448	0.48472	0.16188	0.25706	0.46194	0.13001	0.24569	0.46382	0.09339	0.21755	0.45595
H3	0.64353	0.63630	0.48728	0.66920	0.55709	0.44523	0.59001	0.52841	0.40780	0.58020	0.56463	0.38896	0.58936	0.67520	0.34841

Figure S14. The atom coordinates of computation models in the Figure 4f.

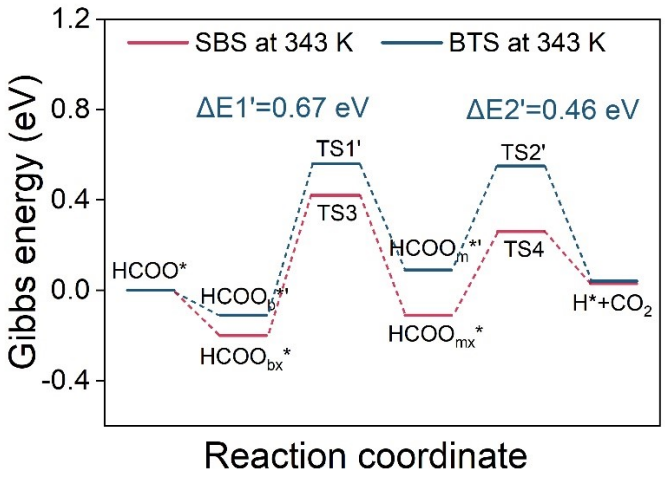

Figure S15. Gibbs free energies of the SBS and the BTS at the same temperature of 343 K.

Table S1. The comparison of reaction conditions between our work and other catalytic systems.

Ref.	FA concentration	Additives	Solvents	Catalysts	TOF
1	1 mol L^{-1} (wt. 4.6%)	None	H_2O	NiPd/NH_2-N-rGO	954.3 h^{-1}
2	1 mol L^{-1} (wt. 4.6%)	None	H_2O	PdAu/HPC-NH_2	3763 h^{-1}
3	2 mol L^{-1} (wt. 9.2%)	None	H_2O	DHBP-Ir	2800 h^{-1}
4	1 mol L^{-1} (wt. 4.6%)	None	H_2O	$PdCl_2$ Acet./Cdarco	4888 h^{-1}
5	1 mol L^{-1} (wt. 4.6%)	None	H_2O	CrPd/MIL-101-NH_2	2009 h^{-1}
6	1 mol L^{-1} (wt. 4.6%)	None	H_2O	AgPd/NH_2-SBA-15	1166 h^{-1}
Our work	**>21.3 mol L^{-1} (wt. >98%)**	**None**	**None**	**Pd/rGO aerogel**	**4672 h^{-1}**

1. J. M. Yan, S. J. Li, S. S. Yi, B. R. Wulan, W. T. Zheng and Q. Jiang, Adv Mater, 2018, 30, e1703038.
2. Z. Wang, S. Liang, X. Meng, S. Mao, X. Lian and Y. Wang, Applied Catalysis B: Environmental, 2021, 291.
3. I. Mellone, F. Bertini, M. Peruzzini and L. Gonsalvi, Catalysis Science & Technology, 2016, 6, 6504-6512.
4. J. L. Santos, C. Megías-Sayago, S. Ivanova, M. Á. Centeno and J. A. Odriozola, Chemical Engineering Journal, 2020.
5. D. Gao, Z. Wang, C. Wang, L. Wang, Y. Chi, M. Wang, J. Zhang, C. Wu, Y. Gu, H. Wang and Z. Zhao, Chemical Engineering Journal, 2019, 361, 953-959.
6. Y. Zhu, T. Nakanishi, K. Kanamori, K. Nakanishi, S. Ichii, K. Iwaida, Y. Masui, T. Kamei, T. Shimada, A. Kumamoto, Y. H. Ikuhara, M. Jeon, G. Hasegawa, M. Tafu, C. W. Yoon and T. Asefa, ACS Applied Materials & Interfaces, 2017, 9, 36-41.